HTS Tape Mechanical Behavior Sensitivity on Material Properties and Thickness of Material Layers

Hamed Milanchian, Tiina Salmi, Alexandre Halbach, and Reijo Kouhia

***Abstract*—Multilayer 2G high-temperature superconductor (HTS) tapes undergo various mechanical loading steps as part of a superconducting magnet operation. The mechanical loading steps include cool-down to cryogenic temperatures and Lorentz forces when powering up the magnets. Studying the mechanical behavior of the constituent layers in a HTS tape can reveal the strain or stress level in each layer and help in predicting the probability of mechanical failure or critical current degradation. A detailed finite element method (FEM)-based simulation models enable us to estimate the mechanical behavior in each layer. However, defining the model parameters for material mechanical properties or thickness of each material layer can have considerable uncertainty due to variation in manufacturing processes and missing measurements of material properties within these tapes. The material properties in thin layers may not exactly comply with bulk materials of the same kind. In this paper we present a sensitivity analysis for mechanical behavior dependence on material properties variation in the constituent layers of a HTS tape. The results give important insight about the accuracy and reliability of mechanical simulation results and guide the priorities in future material characterization. In addition, we will investigate the effect of the thickness of Hastelloy layer on effective macroscopic mechanical behavior of the tape. A nonlinear elastoplastic FEM model is used for performing the simulations.**

***Index Terms*—FEM, HTS tapes, mechanical analysis, YBCO.**

I. Introduction

MULTILAYER Yttrium barium copper oxide (YBCO)-based coated HTS tapes have been regarded as a promising option for future high-field applications [1]. Studying the mechanical behavior of these tapes is very crucial for HTS tape-based cable, coil, and superconductor magnets, as mechanical strain can lead to a degradation of YBCO's critical current [2].

Several mechanical modeling of coated HTS tapes has been done before with different finite element (FE) modeling softwares, Abaqus, Ansys, and COMSOL [3], [4], [5]. A 3D nonlinear numerical FE model for HTS tapes has already been developed by us, which enables studying strain and stress in elastoplastic regimes [6]. This weak formulation FE model has been built in the FEM C++ library of Sparselizard [7]. In addition to the numerical models, one needs to have the correct material properties in order to produce reliable simulation results. These properties are typically not readily available within the temperature range of interest, and material properties can represent one of the biggest uncertainty in the simulation input. In the review presented in [6], it was found that the material properties of the constituent layers in the simulated HTS tapes varied significantly in the literature. Therefore, it is very insightful to know how each material property of each layer affects the study and the simulations. This work utilizes the built FE model and Sparselizard implementation in material property sensitivity analysis impacting the mechanical behavior of HTS tapes and the YBCO layer. Another aspect expected to affect the tape mechanical behavior strongly is the thickness of the substrate (Hastelloy) layer. Hence, in this paper, the Hastelloy thickness impact on the tape and YBCO layer during loadings was quantified as well.

In Section II, the numerical mechanical model is briefly presented. Next, the coated HTS tape, geometry and material properties are explained in Section III. In Section IV, the results, including the material sensitivity analysis and Hastelloy thickness analysis, are demonstrated. Finally, Section V concludes this article.

II. Mechanical Model

The elastic mechanic model is as follows:

$$\nabla \cdot \underline{\boldsymbol{\sigma}} + \vec{b} = 0 \tag{1}$$

$$\underline{\boldsymbol{\sigma}} = \boldsymbol{D} : (\underline{\varepsilon} - \underline{\varepsilon}_{\text{th}}) \tag{2}$$

$$\underline{\varepsilon} = \frac{1}{2}\left(\nabla \vec{u} + (\nabla \vec{u})^T\right). \tag{3}$$

Stress tensor and infinitesimal strain tensor are shown with $\underline{\boldsymbol{\sigma}}$ and $\underline{\varepsilon}$, $\vec{u}$ is the displacement field, and $\underline{\varepsilon}_{\text{th}}$ is the thermal strain caused by temperature change. Moreover, $\vec{b}$ is the body force, and $\boldsymbol{D}$ is the elastic material stiffness tensor.

For implementing an elastoplastic study, a plasticity model should be used. The isotropic linear hardening model has been used for that purpose which includes the additive decomposition rule (4), Hooke's law (5), flow rule (6), isotropic hardening rule

Manuscript received 12 November 2022; revised 10 February 2023; accepted 20 February 2023. Date of publication 1 March 2023; date of current version 15 March 2023. This work was supported by the Academy of Finland, under Grant 324887 (Super20T). *(Corresponding author: Hamed Milanchian.)*

Hamed Milanchian and Tiina Salmi are with the Department of Electrical Engineering, Tampere University, 33720 Tampere, Finland (e-mail: hamed.milanchian@tuni.fi).

Alexandre Halbach is with Quanscient, Tampere, Finland.

Reijo Kouhia is with the Department of Civil Engineering, Tampere University, 33720 Tampere, Finland.

Color versions of one or more figures in this article are available at https://doi.org/10.1109/TASC.2023.3251293.

Digital Object Identifier 10.1109/TASC.2023.3251293

This work is licensed under a Creative Commons Attribution 4.0 License. For more information, see https://creativecommons.org/licenses/by/4.0/

(7), and the consistency condition (8).

$$\dot{\underline{\varepsilon}} = \dot{\underline{\varepsilon}}^{\mathrm{e}} + \dot{\underline{\varepsilon}}^{\mathrm{p}} \tag{4}$$

$$\dot{\underline{\boldsymbol{\sigma}}} = \boldsymbol{D} : (\dot{\underline{\varepsilon}} - \dot{\underline{\varepsilon}}^{\mathrm{p}}) \tag{5}$$

$$\dot{\underline{\varepsilon}}^{\mathrm{p}} = \dot{\lambda} \frac{\partial f}{\partial \underline{\boldsymbol{\sigma}}} = \dot{\lambda}\, \hat{n} \tag{6}$$

$$\dot{K} = H\, \dot{\lambda} \tag{7}$$

$$\dot{f} = 0. \tag{8}$$

In which $\underline{\varepsilon}^{\mathrm{e}}$ and $\underline{\varepsilon}^{\mathrm{p}}$ are the elastic and plastic components of the total strain, λ, and $\hat{n}$ are the plasticity multiplier (norm) and the unit direction vector for it, H is the generalized plastic modulus (related to the tangent modulus), K is the isotropic hardening parameter, and f is the yield function. Note that plastic behavior starts with stress reaching a critical value (yield stress) and causes permanent deformations. The yield function is defined to state if plasticity happened or not. The yield function in the isotropic linear hardening plasticity model considering Von Mises equivalent stress is defined as follows:

$$f = \sqrt{\frac{3}{2}\, \underline{\boldsymbol{s}} : \underline{\boldsymbol{s}}} - \sigma_{\mathrm{y}} - K \qquad \begin{cases} f < 0 & \text{elastic,} \\ f = 0 & \text{plastic.} \end{cases} \tag{9}$$

The deviatoric stress, $\underline{\boldsymbol{s}}$, in (9) can be computed from:

$$\underline{\boldsymbol{s}} = \underline{\boldsymbol{\sigma}} - \frac{1}{3}\mathrm{tr}(\underline{\boldsymbol{\sigma}})\underline{\mathbb{1}}. \tag{10}$$

To solve the nonlinear elastoplastic problem, the FE weak form of the elastic model and the discretized plasticity rules are used together with Newton-Raphson method. The complete formulation has been reported in [6].

III. HTS Tape

The coated HTS tapes are composites with different layers. Copper, Hastelloy, YBCO, silver, and buffer are the main materials.

A tape with all seven layers (including all materials) is considered for the material property sensitivity analysis. For Hastelloy thickness sensitivity analysis, the buffer and silver layers are omitted because, based on the results shown in Section IV-A, they would have negligible impact on the results.

A schematic of the seven-layered tape is shown in Fig. 1. The fixed mechanical boundary condition of one end of the tape has also been shown, and the tape is aligned along the z-axis. The thickness for the layers, width, and length of the simulated tape are in Table I.

For modeling the cool-down and axial loading of the HTS tape with linear hardening elastoplasticity model, elastic properties as young modulus (E), Poisson's ratio (ν), thermal property as the coefficient of thermal expansion ($\underline{\boldsymbol{\alpha}}_{\mathrm{th}}$) and plastic behavior properties as initial yield stress and tangent modulus are required. The material properties in Table II have been chosen for the constituent layers in the HTS tape for the reference case in our simulations. There are uncertainties about the exact behavior of the YBCO layer in the HTS tapes due to the unique manufacturing process and its super thin thickness (2 μm); still, an elastoplastic behavior has been selected for our simulations ($\sigma_{\mathrm{y}} = 40$ MPa, $E_{\mathrm{T}} = 0$). The 40 MPa assumption for σ_{y} is a rough average value based on bulk YBCO measurements, 31 MPa of splitting tensile strength [8], and flexural strength of 54–57 MPa [9]. While in HTS tapes applications, some, such as [10] and [11], considered a yield stress of 56 MPa for the YBCO layer, [4] used complete elastic assumption, and [5] assumed elastoplastic behavior with a yield stress of 1200 MPa.

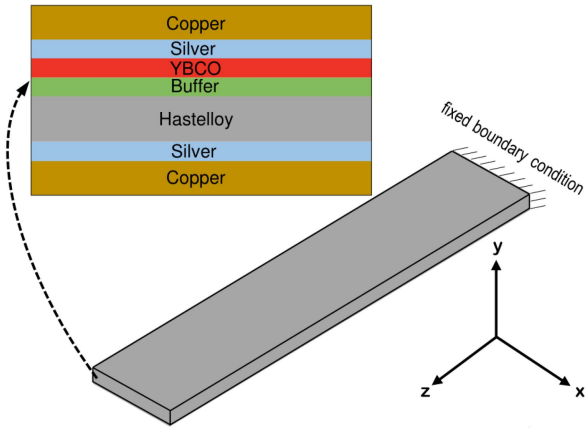

Fig. 1. Schematic of a seven-layered coated HTS tape.

TABLE I
THE SIMULATED HTS TAPE DIMENSIONS [M]

copper	20×10^{-6}
silver	2×10^{-6}
Hastelloy	100×10^{-6}
buffer	1×10^{-6}
YBCO	2×10^{-6}
width	5.3×10^{-3}
length	8×10^{-2}

TABLE II
MATERIAL PROPERTIES OF THE REFERENCE CASE OF THE HTS TAPE

	α_{th} [K^{-1} $\times 10^{-6}$]	E [GPa]	ν	σ_{y} [MPa]	E_{T} [GPa]
copper	17.7	80	0.338	275	4
silver	17	70	0.367	140	0
Hastelloy	13.4	200	0.307	980	8.5
buffer	9.5	170	0.226	40	0
YBCO	11	157	0.3	40	0

IV. Results

The simulation of HTS tapes takes place in two stages of loadings. Initially, the tape is cooled-down to 77 K. The strain

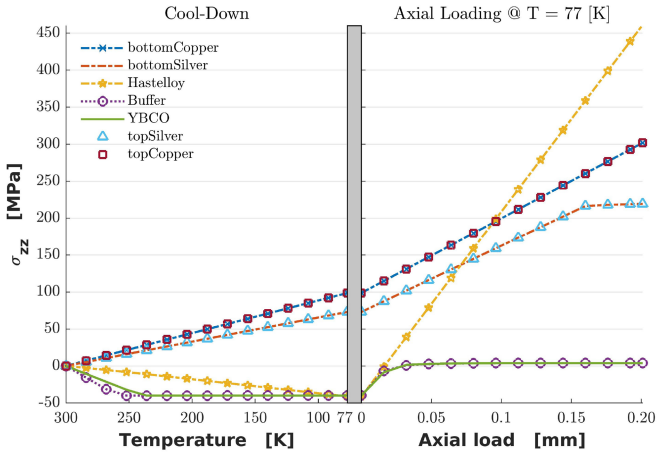

Fig. 2. Stress in constituent layers of the detailed HTS tape (7-layered) during cool-down and axial loading stage (with reference case material properties).

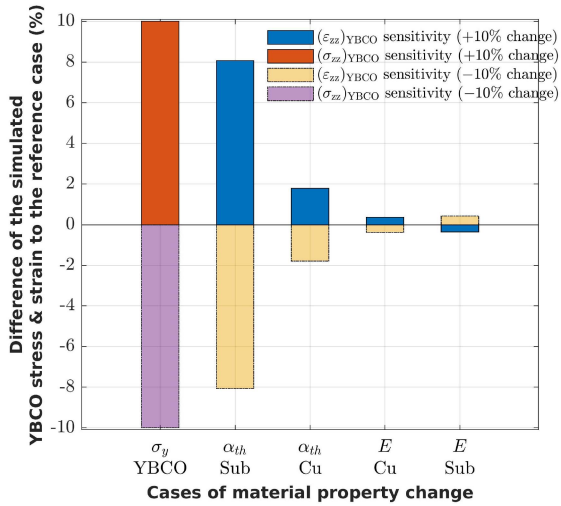

Fig. 3. Relative difference of YBCO layer strain and stress after cool-down in cases of ±10% material property change (top 5 cases).

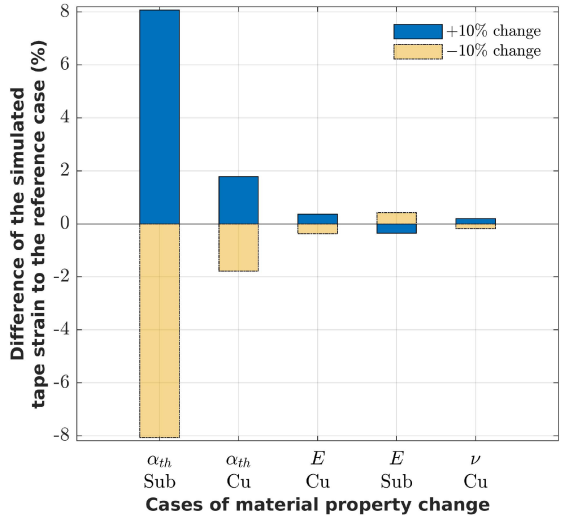

Fig. 4. Relative difference of tape strain after cool-down in cases of ±10% material property change (top 5 cases).

and stress are studied at this point. Later, the axial loading by means of imposed boundary condition is simulated. Note that pre-strain, pre-stress, and plastic material property evolution act as initial conditions prior to studying the axial loading part. As the tape is axially loaded, the strain and stress along the tape (z-axis) are studied in the results. The stress along the tape after both loading for the reference case can be found in Fig. 2. The stress in layers of HTS tape emerges in cool-down due to the difference in thermal properties, and later more stress is generated during axial loading of the tape. The YBCO layer in both loading and the silver layer in axial loading undergo the plasticity regime. The built FE numerical model with Sparselizard has been compared with COMSOL, and a below 0.4% difference has been obtained [6].

A. *Material Sensitivity Analysis*

To investigate the impact of the material properties of the layers on the mechanical study sensitivity analysis has been implemented. With five materials in the tape (copper, silver, Hastelloy, buffer, YBCO), five material properties (α_{th}, E, ν, E_T, σ_{y}), and two change cases (+10% and -10% of change for each material property), there will be 50 different cases of simulations to be executed. Each of the cases is compared with the reference case, and the differences in (1) YBCO behavior and (2) the tape's average behavior are reported. This sensitivity analysis is done once at the cooled-down point and once after axial loading at 77 K. After studying the cases impacting YBCO behavior after cool-down, the results show that the silver and buffer properties had a below 1% effect. The effect of the top five properties of the other three materials is in Fig. 3. As is seen from Fig. 3, YBCO's σ_{y} has 10% effect on $(\sigma_{zz})_{\text{YBCO}}$, Hastelloy's α_{th} and copper's α_{th} have 8% and 2% effect on $(\varepsilon_{zz})_{\text{YBCO}}$. For tape's behavior after the cool-down, silver, buffer, and YBCO properties had below 1% effect. Again top 5 most influential copper and Hastelloy properties impacting tape after cool-down are chosen to be shown in Fig. 4. Hastelloy's α_{th} has the largest effect, with 8% change in $(\varepsilon_{zz})_{\text{tape}}$.

With the assumed elastoplastic behavior and material properties for the YBCO layer, it lies in the perfect plastic regime, and the stress does not evolve during axial loading; therefore, it is not possible to see the difference and do the sensitivity analysis for YBCO behavior during axial loading. On the other hand, the sensitivity analysis impacting tape strain after 600 MPa of axial loading at 77 K has been done. 600 MPa stress was chosen as it is close to 700 MPa of yield stress in SuNam HTS tapes. Similar to cool-down tape analysis, the effect of silver, buffer and YBCO properties are negligible and below 1%. The results of the top 5 properties are in Fig. 5. Hastelloy's E and α_{th} have the most significant effect, 59% in -10% and 48% in +10% change for Young's modulus and 36% difference for the coefficient of thermal expansion impacting $(\varepsilon_{zz})_{\text{tape}}$. Copper's α_{th} and σ_{y} have almost 8% effect on $(\varepsilon_{zz})_{\text{tape}}$ as well.

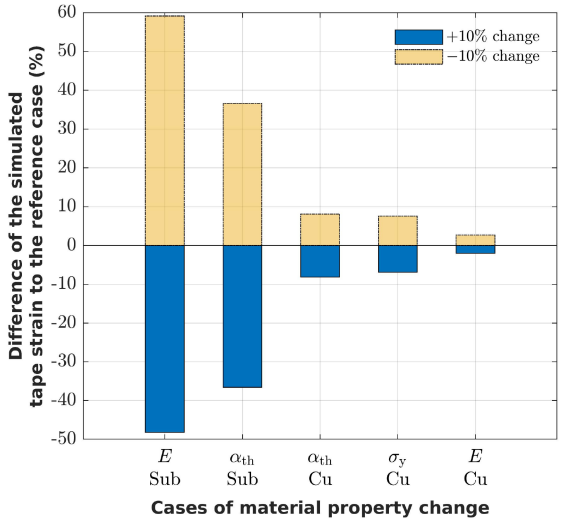

Fig. 5. Relative difference of tape strain after cool-down and 600 MPa of axial loading in cases of $\pm 10\%$ material property change (top 5 cases).

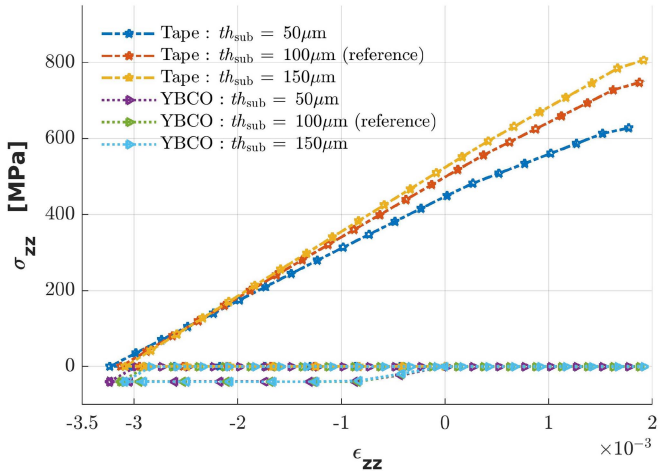

Fig. 6. The strain-stress behavior of the HTS tape and the YBCO layer during cool-down and mechanical loading with different thickness of Hastelloy layer.

B. Hastelloy Thickness Sensitivity Analysis

The Hastelloy layer (the substrate layer in HTS tapes) provides the mechanical stability for the tape and makes most part of it (50–70% in HTS tapes of different manufacturers). The HTS tape's average mechanical behavior depends on this crucial layer. Therefore, how this layer's thickness affects the whole behavior should be studied. The whole loading case for the HTS tape (cool-down + axial loading) with two more different thicknesses of Hastelloy (50 μm and 150 μm) are simulated and compared with the common 100 μm thickness of Hastelloy. The strain-stress diagram for the YBCO layer and tape behavior is shown in Fig. 6. In both cases (50 μm and 150 μm thickness of Hastelloy), the YBCO layer lies in the plasticity regime, similar to the reference case, and not much different behavior can be seen. However, larger impacts on tape behavior can be seen with different thicknesses of Hastelloy. For better comparison, the differences to the HTS reference case of 100 μm thickness of Hastelloy after cool-down and after 600 MPa of axial loading at 77 K are computed, which can be found in Table III. With $\pm 50\%$ of Hastelloy thickness change, below 4% effect has been observed impacting YBCO strain, YBCO stress, and tape strain at the complete cool-down. On the other hand, after 600 MPa of the axial loading, HTS tape with thicker Hastelloy (+50% change) has -33.36% effect impacting tape strain. In addition, the HTS tape with thinner Hastelloy (-50% change) undergoes larger tape strain (102.09%).

TABLE III
RELATIVE DIFFERENCE OF YBCO LAYER AND TAPE AVERAGE BEHAVIOR IN DIFFERENT HASTELLOY THICKNESSES COMPARING TO THE REFERENCE CASE OF 100 μM

	Hastelloy thickness		50 μm	150 μm
Difference to the reference case (%)	complete cool-down (77 K)	$\varepsilon_{\mathrm{YBCO},zz}$	3.34	-1.35
		$\sigma_{\mathrm{YBCO},zz}$	-0.04	0.01
		$\varepsilon_{\mathrm{tape},zz}$	3.34	-1.35
	Axial loding (600 MPa)	$\varepsilon_{\mathrm{tape},zz}$	102.09	-33.36

V. CONCLUSION

Material properties sensitivity analysis was done for coated HTS tape mechanical simulation during cool-down and axial loading. The results suggested that Hastelloy's E and α_{th} had the largest impact on the simulated loadings. For example, a 10% decrease in Hastelloy's E led to a 58% increase in tape strain. Regarding the YBCO layer behavior, especially its transition to the plastic regime, σ_{y} obviously is essential. However, finding a reliable value for the yield stress value of the thin YBCO layer in the literature is not easy. As expected, the thin silver and buffer layers had almost no impact on the study. Consequently, when selecting the material properties, one should pay the most attention in choosing the properties for Hastelloy. YBCO mechanical characterization is also required for future works to obtain more accurate results that may be needed for YBCO delamination and critical current degradation analyses.

The Hastelloy thickness sensitivity analysis considered 50 μm, 100 μm, and 150 μm of Hastelloy thicknesses. After the cool-down, all cases behave rather similarly. After subsequent axial loading, the 50 μm thick Hastelloy tape had 102% and 136% more strain than the 100 μm and the 150 μm thick Hastelloy tapes. The thicker Hastelloy in tapes thus decreases the strain in the tape and the YBCO layer when subject to the same axial loading. This could be one aspect to consider when designing the architecture of a coated HTS tape for a given application.

REFERENCES

[1] W. H. Fietz, M. J. Wolf, A. Preuss, R. Heller, and K.-P. Weiss, "High-current HTS cables: Status and actual development," *IEEE Trans. Appl. Supercond.*, vol. 26, no. 4, Jun. 2016, Art. no. 4800705.

[2] J. S. Murtomäki et al., "Investigation of REBCO Roebel cable irreversible critical current degradation under transverse pressure," *IEEE Trans. Appl. Supercond.*, vol. 28, no. 4, 2018, Art. no. 4802506.

[3] K. Ilin et al., "Experiments and Fe modeling of stress–strain state in REBCO tape under tensile, torsional and transverse load," *Supercond. Sci. Technol.*, vol. 28, no. 5, 2015, Art. no. 055006.

[4] N. Allen, L. Chiesa, and M. Takayasu, "Structural modeling of HTS tapes and cables," *Cryogenics*, vol. 80, pp. 405–418, 2016.

[5] P. Gao, W.-K. Chan, X. Wang, Y. Zhou, and J. Schwartz, "Stress, strain and electromechanical analyses of (RE) $\mathrm{Ba_2Cu_3O}_x$ conductors using three-dimensional/two-dimensional mixed-dimensional modeling: Fabrication, cooling and tensile behavior," *Supercond. Sci. Technol.*, vol. 33, no. 4, 2020, Art. no. 044015.

[6] H. Milanchian, T. Salmi, A. Halbach, and R. Kouhia, "Thermo-elasto-plastic analysis of coated high temperature superconductor tapes using open source FEM library of Sparselizard," unpublished, 2022.

[7] A. Halbach, "Sparselizard - The user friendly finite element C++ library," 2017. [Online]. Available: https://sparselizard.org/

[8] K. Konstantopoulou, Y. Shi, A. Dennis, J. Durrell, J. Pastor, and D. Cardwell, "Mechanical characterization of GDBCO/AG and YBCO single grains fabricated by top-seeded melt growth at 77 and 300 k," *Supercond. Sci. Technol.*, vol. 27, no. 11, 2014, Art. no. 115011.

[9] K. Konstantopoulou, "Mechanical behavior of 2 G REBCO HTS at 77 and 300 k," Ph.D. dissertation, Caminos, 2015.

[10] J. R. C. Dizon, A. B. Gorospe, and H.-S. Shin, "Numerical analysis of stress distribution in Cu-stabilized GDBCO CC tapes during anvil tests for the evaluation of transverse delamination strength," *Supercond. Sci. Technol.*, vol. 27, no. 5, 2014, Art. no. 055023.

[11] L. Liu, Y. Zhu, X. Yang, T. Qiu, and Y. Zhao, "Delamination properties of YBCO tapes under shear stress along the width direction," *IEEE Trans. Appl. Supercond.*, vol. 26, no. 6, Sep. 2016, Art. no. 6603406.